

Direct link between boson-peak excess vibrational modes and α -relaxation in glasses

Bingyu Cui^{1,2}, Rico Milkus¹, Alessio Zaccone^{1,3}

¹*Statistical Physics Group, Department of Chemical Engineering and Biotechnology, University of Cambridge, New Museums Site, CB2 3RA Cambridge, U.K.*

²*Department of Applied Mathematics and Theoretical Physics, University of Cambridge, Wilberforce Road, Cambridge CB3 0WA, U.K. and*

³*Cavendish Laboratory, University of Cambridge, JJ Thomson Avenue, CB30HE Cambridge, U.K.*

We implemented the vibrational density of states (DOS) of a disordered lattice of elastically-bound spherical particles (to represent partial charges, in our case) in the general Lorentz sum rule for the dielectric response. Focusing on systems right at the glass transition temperature, we selected the vibrational density of states of a marginally stable disordered lattice, which features a strong boson peak (excess of soft modes over Debye $\sim \omega_p^2$ law), and compared the calculated dielectric function with experimental data for the paradigmatic case of glycerol at $T \lesssim T_g$. Good agreement is found for both the reactive (real part) of the response and for the α -relaxation peak in the imaginary part, with a significant improvement over earlier theoretical approaches in the reactive modulus. On the low-frequency side of the α -peak, the absence of phonon-like continuum modes due to mechanical instability right at the glass transition explains the linear $\sim \omega$ scaling observed in experiments. α -wing asymmetry and stretched-exponential behaviour are recovered on the high-frequency side of the peak, and in the time-domain, respectively, and are shown to be directly caused by the soft boson-peak modes.

I. INTRODUCTION

Supercooled liquids that undergo a liquid-glass transition exhibit an abrupt and dramatic slowdown of the atomic/molecular dynamics upon approaching the glass transition temperature T_g [1–4]. The α -relaxation describes the slowest component of the time-relaxation (or autocorrelation function) of material response, including mechanical relaxation, relaxation of density fluctuations or of the dielectric polarization [5]. The α -relaxation phenomenon has always been associated with the collective and strongly cooperative motion of a large number of atoms/molecules which rearrange in a long-range correlated way [1]. This process has also been interpreted, within the energy landscape picture, as the transition of the system from one meta-basin to another, which involves the thermally activated jump over a large energy barrier [6–8].

Modern theories of dielectric response of matter [9, 10] are based on the Lorentz model [11, 12], which approximates electrons as classical particles bound harmonically to positive background charges. Upon assuming that all oscillators move at the same natural frequency, the relaxation function $\epsilon(t)$ is a simple-exponential increasing function of time, while the imaginary part $\epsilon''(\omega)$ of the complex dielectric function $\epsilon^*(\omega)$, features a resonance peak given by a Lorentzian function [11, 12].

Correcting to account for the rotational Brownian motion in the case of strongly anisotropic molecules, as in the Debye dielectric-relaxation theory [9], does not alter the simple-exponential relaxation. While this may be a good approximation for gases and high- T liquids, it is not valid for glasses, as is well known since the time of Kohlrausch [13, 14]. For supercooled liquids in general, and for glasses in particular, the Kohlrausch stretched-

exponential function $\sim \exp[-(t/\tau)]^\beta$ provides a good empirical fit of the relaxation function and of the dielectric loss [1, 2, 5, 15–17].

Mode-coupling theory (MCT) developed by W. Goetze and co-workers, has provided a general interpretation of the α -peak in dielectric relaxation using a framework where the many-body microscopic dynamics of charges is treated statistically, in the same way as for an ensemble of classically interacting spherical particles [4]. The most striking success of MCT has been the first-principles derivation of the Kohlrausch stretched-exponential relaxation for α -relaxation in the liquid phase.

While MCT has had tremendous success in describing supercooled liquids at $T > T_g$, the situation is quite different at $T \simeq T_g$ or in the glass at $T < T_g$. Here, although MCT provides a theoretical foundation for Kohlrausch stretched-exponential behaviour, direct comparisons with experimental data have not been possible due to the difficulty of calibrating various parameters in the theory. This scenario is the most striking for the paradigmatic case of glycerol: this is the most widely studied organic glass-former in the experimental literature, yet no microscopic theory has been used to describe the dielectric response of this material apart from empirical models (e.g. Havriliak-Negami), which have no physics in them.

Here we take a very different approach: instead of the liquid-state approach of MCT, we take the opposite point of view, and describe the dynamics in analogy with a disordered solid-state lattice of particles which perform harmonic oscillations. Due to the disorder in the lattice (and in particular due to the absence of local inversion symmetry [18]), the low-frequency part of the vibrational density of states (DOS) is dominated by an excess of soft modes over the Debye ω_p^2 law valid for crystals.

This excess of soft modes in the DOS is universally known in the literature on glassy physics and disordered systems as the "boson peak" [19–22]. In the following we use this terminology and we refer to the broad ensemble of all these excess soft modes over Debye ω_p^2 law as the boson peak. It is important to note that, in the sub-field of dielectric spectroscopy of glasses, the terminology "boson peak" is used to designate an isolated peak in the THz frequency regime of the dielectric loss modulus ϵ'' . In our work we will never refer to or consider this THz-frequency peak in the loss modulus, so there is no ambiguity in our terminology and the term "boson peak" is used exclusively to designate the ensemble of excess non-Debye modes in the low- ω_p part of the vibrational DOS.

Famous physicists in the past have attempted to explain stretched-exponential relaxation (which is the hallmark of the α -relaxation in glasses) in terms of the underlying cooperative coupling of vibrational degrees of freedom [15–17]. In spite of these efforts, the link between quasi-localized soft vibrational modes or boson peak modes in the DOS, and the α -relaxation process, has surprisingly received less attention, with important exceptions like Ref. [23] and the macroscopic model for viscoelasticity of Ref. [24]. This is despite the fact that both the boson peak in the vibrational DOS and the α -relaxation process display a strong T -dependence near T_g (for the T -dependence of the boson peak, see e.g. [25, 26]).

Although Kohlrausch stretched-exponential relaxation has been reported also below T_g [27], this behaviour cannot be explained with MCT which is only valid at $T > T_g$. For the first time, we provide a simple and explicit set of relations between the dielectric relaxation functions and the DOS of disordered lattices, which gives rise to the observed stretched-exponential relaxation in time and to the α -relaxation peak in the loss modulus of glycerol at $T \lesssim T_g$. An excellent agreement is found for the reactive modulus, whereas the loss modulus agreement has to be improved by refining the model with a more realistic DOS (e.g from atomistic simulations) for glycerol in future studies.

II. EXTENDED THOMSON-LORENTZ MODEL OF DIELECTRIC RESPONSE

In the following, we work within the Thomson-Lorentz plum-pudding model of disordered elastically bound classical charges (basically on the same general coarse-graining level as in Ref. [3]). Within the Lorentz sum rules, we make use of a DOS $\rho(\omega_p)$ obtained by numerical diagonalization of a model random lattice of harmonically-bound spherical particles obtained by driving a dense Lennard-Jones system into a metastable glassy energy minimum with a Monte-Carlo relaxation algorithm, and then replacing all the nearest-neighbour pairs with harmonic springs all of the same length and spring constant [18]. Springs are then cut at random

in the lattice to generate random network lattices with variable mean coordination Z , from $Z = 9$ down to the isostatic limit $Z = 2d = 6$. It is important to notice that this simplified model DOS is convenient for its simplicity and to single-out generic features of glassy behaviour, but in order to obtain very accurate fittings more realistic simulated DOS (e.g. from molecular simulations) will be employed in the future.

A. Vibrational DOS and its T -dependence

The DOS obtained from numerical diagonalization of the simulated network is expressed in terms of dimensionless eigenfrequencies ω_p . Generally, the eigenfrequency ω_p obtained from numerics and the eigenfrequency ω'_p of the *real* experimental systems are related via $\omega'_p \approx \sqrt{\kappa/m}\omega_p$ where m is the effective mass of the charged particle and κ the spring constant, under the condition that $\int_0^{\omega_p^D} \rho'(\omega'_p) d\omega'_p = \int_0^{\omega_p^D} \rho(\omega_p) d\omega_p$. We use the constant $C = \sqrt{\kappa/m}$ as a fitting parameter. κ and m are both equal to unity in the numerical simulation of the DOS, whereas their values are of course different for different experimental systems (in the case of dielectric response, m is to understood as an effective mass).

Also, the DOS obtained from diagonalization of the model random networks, depends on the average coordination number Z . For example, the boson peak frequency drifts towards lower values of ω_p according to the scaling $\omega_p^{BP} \sim (Z - 6)$. Hence, Z is the crucial control parameter of the relaxation process which in a real molecular glass changes with T . Therefore, in order to use our numerical DOS data in the evaluation of the dielectric function, we need to find a physically meaningful relation between Z and T at the glass transition. Within this picture, Z represents the effective number of intermolecular contacts, which increases the number of positive charges to which a negative charge is bound in the material.

In all experimental systems which measure the T -dependent material response, the temperature is varied at constant pressure, which implies that thermal expansion is important. Following previous work, we thus employ thermal expansion ideas [28] to relate Z and T . Upon introducing the thermal expansion coefficient $\alpha_T = \frac{1}{V}(\partial V/\partial T)$ and replace the total volume V of the sample via the volume fraction $\phi = vN/V$ occupied by the molecules (v is the volume of one molecule), upon integration we obtain $\ln(1/\phi) = \alpha_T T + const$. Approximating $Z \sim \phi$ locally, we get $Z = Z_0 e^{-\alpha_T T}$. Imposing that $Z_0 = 12$, as for FCC crystals at $T = 0$ in accordance with Nernst principle, we finally get, for glycerol, $Z \approx 6.02$ when $T = 184K$. This is very close to the reported T_g for this material [27].

It is seen in Fig.1 and in Fig. 2 that for the case $Z = 6.1$, i.e. very close to the solid-liquid (glass) transition that occurs at $Z = 6$, a strong and broad boson peak is present in the DOS. Upon increasing Z towards higher

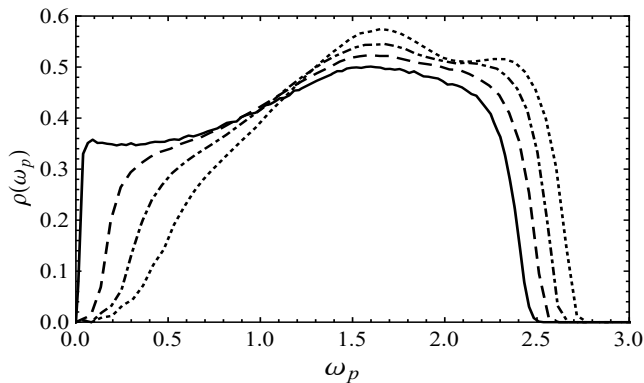


FIG. 1. Density of states (DOS) with respect to eigenfrequency ω_p at $Z = 6.1$ (solid line), i.e. close to the marginal stability limit $Z = 6$ that we identify here as the solid-liquid (glass) transition; plots of the DOS at $Z = 7$, $Z = 8$, $Z = 9$ are also shown, and are marked as dashed, dot dashed and dotted lines, respectively.

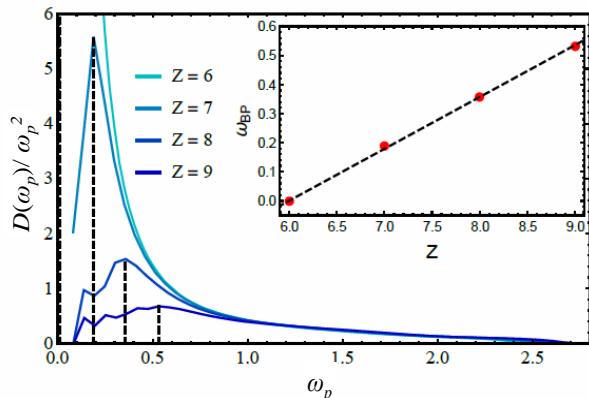


FIG. 2. The DOS normalized by Debye's ω_p^2 law, for (from bottom to top): $Z = 9$, $Z = 8$, $Z = 7$, $Z = 6$, which gives evidence of the boson peak at low ω_p . The eigenfrequency of boson peak scales as $\omega_p^{BP} \sim (Z - 6)$ as known from work for disordered systems with central-force interactions [18, 21].

values the boson peak is still present but its amplitude decreases markedly upon increasing Z . At $Z = 6.1$, the continuum Debye regime $\sim \omega_p^2$ is not visible or absent, whereas a very small gap between $\omega_p = 0$ and the lowest eigenfrequency exists. Hence, under conditions close to the glass transition where the system loses its shear rigidity, the vibrational spectrum is dominated by a large and broad excess of soft modes with respect to Debye $\sim \omega_p^2$ law at low frequency.

B. Dielectric response as a function of the vibrational DOS

In order to determine the dependence of the polarization and of the dielectric function on the frequency of the field, we have to describe the displacement \underline{r} of each molecule from its own equilibrium position under the applied field \underline{E} . Upon treating the dynamics classically, the equation of motion for a charge i under the forces coming from interactions with other charges and from the applied electric field, is given by the following phenomenological Lorentz damped oscillator equation [11]

$$m\ddot{\underline{r}}_i + \nu\dot{\underline{r}}_i + \underline{H}_{ij}\underline{r}_j = q\underline{E} \quad (1)$$

where m is the (effective) mass of the charged group, and q is its net electric charge. The Hessian $\underline{H}_{ij} = \partial U / \partial \underline{r}_i \partial \underline{r}_j$, where U is the total potential energy of the system, represents the restoring attractive interactions from oppositely-charged nearest-neighbour charges, that tend to bring the charge i back to the rest position that i had at zero-field. ν is a phenomenological damping coefficient due to local frictional collisions in the dense glassy environment. To solve this equation, the first step is to take the Fourier transform: $\underline{r}_i(t) \rightarrow \tilde{\underline{r}}_i(\omega)$, resulting in the equation:

$$-m\omega^2\tilde{\underline{r}}_i + i\nu\omega\tilde{\underline{r}}_i + \underline{H}_{ij}\tilde{\underline{r}}_j = q\tilde{\underline{E}}. \quad (2)$$

We then implement normal-mode decomposition: $\tilde{\underline{r}}_i(\omega) = \hat{\underline{r}}_p(\omega)\underline{\mathbf{v}}_i^p$, and the equation reduces to

$$-m\omega^2\hat{\underline{r}}_p + i\nu\omega\hat{\underline{r}}_p + m\omega_p^2\hat{\underline{r}}_p = q\tilde{\underline{E}},$$

which is solved by $\hat{\underline{r}}_p(\omega) = -\frac{q\tilde{\underline{E}}}{m\omega^2 - i\nu\omega - m\omega_p^2}$. Upon summing the two contributions, the total displacement expressed as a sum over the $k = 1 \dots 3N$ normal modes thus reads

$$\delta\hat{\underline{r}}_i(\omega) = -\sum_{k=1}^{3N} \frac{q}{m\omega^2 - i\nu\omega - m\omega_{p,k}^2} \tilde{\underline{E}}(\omega) \quad (3)$$

where $\omega_{p,k}$ denotes the k -th normal mode frequency.

Each particle contributes to the polarization a moment $\underline{p}_i = q\delta\underline{r}_i$. In order to evaluate the macroscopic polarization using Eq. (3), we need to add together the contributions from all molecular degrees of freedom in the system, $\underline{P} = \sum_i \underline{p}_i$. In order to this analytically, we use the standard procedure of replacing the discrete sum over the total $3N$ degrees of freedom of the solid with the continuous integral over the eigenfrequencies ω_p , $\sum_k \dots = \sum_{\alpha=1}^3 \sum_{i=1}^N \dots \rightarrow \int \rho(\omega_p) \dots d\omega_p$, which gives the following sum rule in integral form for the polarization in glasses

$$\tilde{\underline{P}}(\omega) = -\left[\int_0^{\omega_D} \frac{\rho(\omega_p)q^2}{m\omega^2 - i\nu\omega - m\omega_p^2} d\omega_p \right] \tilde{\underline{E}}(\omega). \quad (4)$$

Here, $\rho(\omega_p)$ is the vibrational DOS, and ω_D is the cut-off Debye frequency arising from the normalization of the density of states. The complex dielectric permittivity ϵ^* is defined as $\epsilon^* = 1 + 4\pi\chi_e$ where χ_e is the dielectric susceptibility which connects polarization and electric field as [11]: $\underline{P} = \chi_e \underline{E}$. Hence, we obtain the complex dielectric function expressed as a frequency integral as

$$\epsilon^*(\omega) = 1 - \int_0^{\omega_D} \frac{A\rho(\omega_p)}{\omega^2 - i(\nu/m)\omega - C^2\omega_p^2} d\omega_p \quad (5)$$

where A is an arbitrary positive constant, ν is the microscopic damping parameter for charge mobility, $C = \sqrt{\kappa/m}$, and ω_D is the Debye cut-off frequency (i.e. the highest eigenfrequency in the vibrational DOS spectrum). As one can easily verify, if $\rho(\omega_p)$ were given by a Dirac delta, one would recover the standard simple-exponential (Debye) relaxation [11]. Note that the theory can be extended to deal with molecules that have stronger inner polarizability by replace previous field \underline{E} with local electric field \underline{E}_{loc} . The detailed derivation is provided in Appendix A. However, it turns out that, this qualitative predictions are not very different from the basic theory without Lorentz field.

It is important to emphasize that, in Eq.(5), low-frequency soft modes which are present in $\rho(\omega_p)$ necessarily play an important role also at low applied-field frequencies ω , because of the ω^2 term in the denominator. As we will see below, this fact in our theory implies a direct role of the boson peak on the α -relaxation process.

C. Finite-size effects in the DOS

Since we are using a DOS obtained numerically from a system with a finite (~ 4000) number of particles in simulations, it is important to correctly take care of finite size effects in Eq.(5). In numerical simulations, the DOS $\rho(\omega_p)$ is not a continuous function, but discrete and can be conveniently represented as $\rho(\omega_p) = \frac{1}{3N} \sum_{k=1}^{3N} \delta(\omega_p - \omega_{p,k})$. Thus, we rewrite Eq.(5) as a sum rule over a discrete distribution of $\omega_{p,k}$:

$$\epsilon^*(\omega) = 1 - \sum_k \frac{A}{\omega^2 - i(\nu/m)\omega - C^2\omega_{p,k}^2} \quad (6)$$

where A has absorbed the scaling constant and $\omega_{p,k}$ denotes the eigenfrequency associated with the k -th normal mode. Since the dielectric function is a complex quantity, we can split it into its real and imaginary parts, i.e. $\epsilon^*(\omega) = \epsilon'(\omega) - i\epsilon''(\omega)$:

$$\epsilon'(\omega) = \epsilon'(\infty) + \sum_k \frac{A_1(C^2\omega_{p,k}^2 - \omega^2)}{(C^2\omega_{p,k}^2 - \omega^2)^2 + (\omega\nu/m)^2}, \quad (7)$$

$$\epsilon''(\omega) = \sum_k \frac{A_2(\omega\nu/m)}{(\omega^2 - C^2\omega_{p,k}^2)^2 + (\omega\nu/m)^2}, \quad (8)$$

Here, $A_1, A_2, \epsilon'(\infty)$ are re-scaling constants that have to be calibrated in the comparison with experimental data. In particular, it is important to note that the experimental data of dielectric permittivity and dielectric loss are not necessarily given in the same units and there is, in general, no coherence between the offsets in the plots of the ϵ' and ϵ'' curves. For this reason, the values of A_1 and A_2 do not necessarily coincide.

As remarked above and as observed in all numerical calculations of the DOS in the vicinity of the mechanical stability point of disordered solids, there exists a lowest non-zero eigenfrequency $\omega_{p,min}$, and a vanishingly small gap between $\omega_p = 0$ and $\omega_{p,min} = 0.00036$. Therefore, when $\omega \ll \omega_{p,min}$, $\epsilon''(\omega)$ becomes

$$\epsilon'' \approx \sum_k \frac{A_2\omega\nu/m}{C^4\omega_{p,k}^4} \sim \omega. \quad (9)$$

III. APPLICATION TO EXPERIMENTAL DATA

We now present our theoretical fittings of state-of-the-art experimental data [27, 29] on glycerol at $T \approx T_g$ using Eq.(7)-(8), also in comparison with the empirical best-fitting Kohlrausch stretched-exponential relaxation fitting. In Fig. 3 we plotted the comparisons for $\epsilon'(\omega)$ at $T = 184 K$, i.e. slightly below T_g , obtained by implementing the numerical DOS of Fig.1 for $Z = 6.1$ in Eq.(7). In this case, it is clear that our theoretical model performs significantly better than the Kohlrausch best-fitting (that is optimized for the joint the fitting of dielectric loss below). This suggests that excess soft modes are important for the fitting of the dielectric response at the glass transition.

In Fig. 4 we present fittings of the dielectric loss, $\epsilon''(\omega)$. In this case it is seen that our theory, given by Eq. (8), provides a reasonably good fitting of the α -peak on both the left-hand and the right-hand side of the peak, and the overall quality of the fitting is comparable to the one of the Kohlrausch best empirical fitting. Our theoretical model provides the crucial connection between the salient features of the DOS near T_g and the corresponding features of the response. Of course, at the higher-frequency end of the α -wing, other effects may as well be important which are not described by our model: in particular, the existence of Johari-Goldstein β -relaxation-type contributions to the loss modulus in this regime has been shown for a variety of systems [30–34].

On the left-hand ascending side of the peak, our model is dominated by the vanishingly small gap between the zero-modes and the lowest boson-peak eigenmode $\omega_{p,min} = 0.00036$, which leads to the power-law, $\sim \omega^1$ as derived in Eq.(9), for the ascending part of the peak. On the high- ω side of the peak, where the dynamics is dominated by the soft boson-peak modes and the

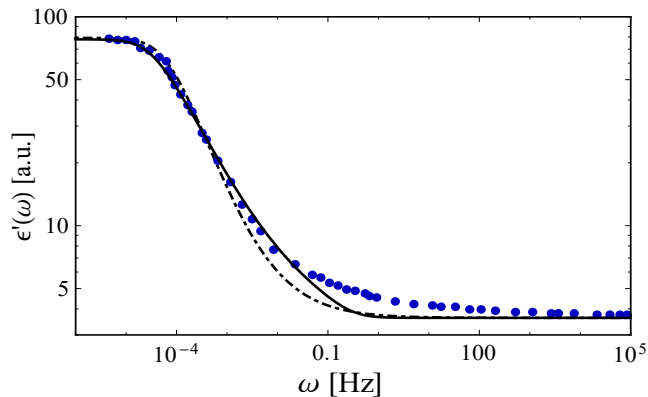


FIG. 3. Real part of the dielectric function as a function of the frequency of the applied field. Symbols are experimental data of the real part of the dielectric function of glycerol at $T = 184\text{ K}$ from Ref. [29]. The solid line is our theory, Eq. (7). The dashed line is the real part of the Fourier transform when we consider the best-fitting (empirical) stretched-exponential function with $\beta = 0.65$. We have taken $C = 10, \nu/m = 1620$ and $A_1 = 0.039$. For the empirical fitting with $\beta = 0.65$, $\tau = 6555$. A rescaling constant is used to adjust the height of the curves.

DOS is approximately flat as a function of ω_p in Fig.1, our model, reproduces, remarkably, the α -wing behaviour still in good agreement with the experimental data.

IV. DIELECTRIC RELAXATION IN THE TIME DOMAIN

We are also interested in the dielectric response in the time domain. The time dependent dielectric function $\epsilon(t)$ and complex dielectric function $\epsilon^*(\omega)$ are related as:

$$\frac{d\epsilon(t)}{dt} = \frac{1}{2\pi} \int_{-\infty}^{\infty} (\epsilon^*(\omega) - \epsilon(\omega = \infty)) e^{i\omega t} d\omega \quad (10)$$

$$\epsilon^*(\omega) = \epsilon(\omega = \infty) - \int_0^{\infty} \frac{d\epsilon(t)}{dt} e^{-i\omega t} dt \quad (11)$$

By using Eq.(5), we can write the analytical form of $\epsilon(t)$ as follows (see Appendix B for the details of the derivation):

$$\epsilon(t) = B + \int_0^{\omega_D} \frac{A\rho(\omega_p)}{2K} \left(\frac{e^{(K-\nu/2m)t}}{K - \nu/2m} + \frac{e^{-(K+\nu/2m)t}}{K + \nu/2m} \right) d\omega_p, \quad (12)$$

where $K \doteq \sqrt{(C\omega_p)^2 - \frac{\nu^2}{4m^2}}$, while B is a re-scaling constant. This equation is a key result: it provides a direct and quantitative relation between the macroscopic relaxation function of the material and the DOS. As we show below, the presence of a boson peak in $\rho(\omega_p)$ directly causes stretched-exponential decay in $\epsilon(t)$ via Eq.(12).

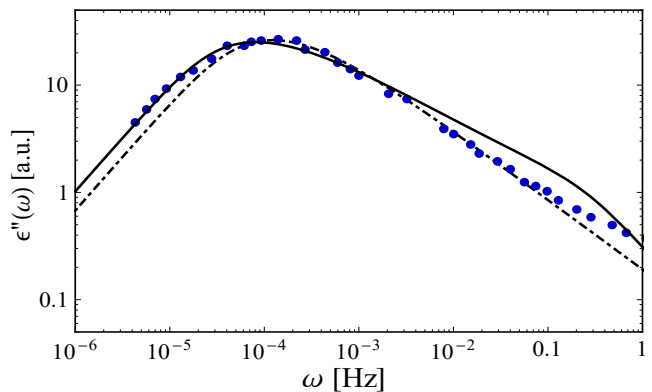


FIG. 4. Dielectric loss modulus as a function of the frequency of the applied field. Symbols are experimental data of the imaginary part of dielectric function of glycerol at $T = 184\text{ K}$ from Ref. [29]. The solid line is the theory presented in this work. The dashed line is the imaginary part of the Fourier transform when we consider the best-fitting (empirical) stretched exponential (Kohlrausch) function with $\beta = 0.65$. In our theory, we have taken $C = 10, \nu/m = 1620$ and $A_2 = 0.0437$ in Eq. (8). For the empirical fitting $\beta = 0.65, \tau = 6555$. A rescaling constant is used to adjust the height of the curves.

In Fig. 5, we plot predictions of Eq.(12) with the parameters calibrated in the glycerol data fitting, along with the Kohlrausch function [35, 36], for the relaxation in the time domain. It is seen that our theory based on soft modes is able to perfectly recover stretched-exponential relaxation, with stretching-exponent $\beta = 0.56$, over many decades in frequency. Without the boson-peak modes in the DOS, we have checked that stretched-exponential relaxation cannot be recovered, and the decay is simple-exponential. Hence, our Eq.(12) provides the long-sought cause-effect relationship between soft modes and stretched-exponential relaxation.

V. CONCLUSIONS

We have re-considered the nature of the α -relaxation peak of simple glass-formers from the standpoint of soft modes and lattice dynamics, as opposed to the traditional views based on MCT and liquid-state concepts. We started from the same presumption of Ref. [3] that dielectric α -relaxation emerges from many-body dynamics in a statistical way, transcending the details of charge dynamics. This should especially be true for glycerol, a paradigmatic glass-forming molecule. With our microscopic framework we are able to reproduce the dielectric response of glycerol in reasonable agreement with state-of-the-art experimental data. Our physically-informed theoretical fitting compares well with empirical Kohlrausch fittings. For the reactive modulus $\epsilon'(\omega)$, our model provides a significantly better fitting than the

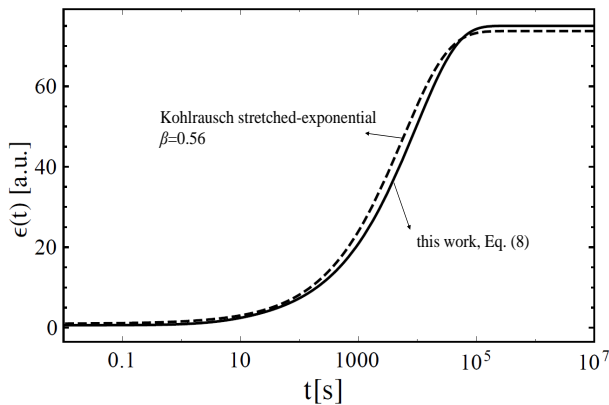


FIG. 5. Time-dependent dielectric response. The solid line is calculated from our theory using Eq.(12) with physical parameters calibrated in the fitting of Fig.3. The dashed line represents the stretched-exponential Kohlrausch function that more closely approximates our theory, calculated using the parameters $\beta = 0.56$ and $\tau = 5655$. Rescaling constants are used to adjust the height of the curves.

best Kohlrausch fitting. For the loss modulus, our model fitting is able to reproduce the α -wing asymmetry although the fit is not perfect in the high-frequency end of the peak, and this could be improved in future work using a more realistic calculation of the DOS for the specific material. For the loss modulus $\epsilon''(\omega)$, on the low-frequency side of the α -peak, we show that the response is controlled by the absence of the continuum $\sim \omega_p^2$ Debye modes in the DOS. The high- ω side of the peak (α -wing) is instead related, within our model, to the boson-peak excess (over Debye) modes in the DOS, where the DOS is nearly flat with respect to the eigenfrequency due to the approach of mechanical instability at the glass transition. In the time-domain response, remarkably, our theory recovers a stretched-exponential relaxation with $\beta = 0.56$, over the entire time domain. These unprecedented results show, for the first time, that stretched-exponential relaxation in glasses is directly caused by the quasi-localized boson-peak excess modes contribution to the relaxation spectrum. These results open up new opportunities to understand the crucial link between α -relaxation, boson peak and dynamical heterogeneity [38, 39] in glasses.

ACKNOWLEDGMENTS

Many useful discussions with R. Richert, W. Goetze, and with E. M. Terentjev are gratefully acknowledged.

Appendix A: local field effect on the total polarization

We consider a spherical cavity around the give molecule such that the general dielectric outside the cav-

ity can be replaced by a system of bound charges. Then we write

$$\underline{E}_{loc} = \underline{E}_0 + \underline{E}_d + \underline{E}_s + \underline{E}_{near}, \quad (\text{A1})$$

where \underline{E}_0 is the external field, \underline{E}_d is the depolarizing field generated by the bound charges on the outer surface of the dielectric medium, \underline{E}_s is the field due to bound charges on the surface of the cavity and \underline{E}_{near} comes from the configuration of all nearby molecules[40]. We have $\underline{E}_d = -4\pi\underline{P}$ since the normal component of the displacement \underline{D} is continuous across the vacuum-dielectric boundary (this claims $\underline{D} = \underline{E}_0 = \underline{E} + 4\pi\underline{P}$) and assume \underline{E}_{near} vanishes in a system where dipoles distributes randomly in uncorrelated positions. We then have

$$\underline{E}_{loc} = \underline{E} + \frac{4\pi}{3}\underline{P}, \quad (\text{A2})$$

in which we used the fact that spherical polarization field impose $E_s = \frac{4\pi}{3}\underline{P}$.

With \underline{E} replaced by \underline{E}_{loc} , we now write equation of motion (1) as

$$m\ddot{\underline{r}}_i + \nu\dot{\underline{r}}_i + \underline{H}_{ij}r_j = q(\underline{E} + \frac{4\pi}{3}\underline{P}). \quad (\text{A3})$$

As a consequence, we instead have

$$\delta\hat{\underline{r}}(\omega) = -\sum_{k=1}^{3N} \frac{q}{m\omega^2 - i\nu\omega - \omega_{p,k}^2} (\tilde{\underline{E}}(\omega) + \frac{4\pi}{3}\tilde{\underline{P}}(\omega)) \quad (\text{A4})$$

If we have $N_0 = V/N$ unite cells per unit volume, the macroscopic polarization is

$$\underline{P} = N_0(q\delta\underline{r} + \alpha E_{local}) \quad (\text{A5})$$

where α is the electronic polarizability[41]. Combining (A2), (A4) and (A5) together, we obtain

$$\epsilon(\omega) = 1 + 4\pi \frac{\chi(\omega)}{\frac{V}{N} - \frac{4\pi}{3}\chi(\omega)},$$

$$\chi(\omega) = q^2 \int_0^{\omega_D} \frac{\rho(\omega_p)}{m\omega^2 - m\omega_p^2 + i\omega\nu} d\omega_p + \alpha \quad (\text{A6})$$

where we have used $\underline{D} = \epsilon\underline{E} = \underline{E} + 4\pi\underline{P}$.

Appendix B: Derivation of Eq.(12) for the relaxation function in the time-domain

We recall that the Fourier transform of a function $f(x)$, in this article, is defined as:

$$\hat{f}(\omega) = \int_{-\infty}^{\infty} f(x)e^{-i\omega x} dx \quad (\text{B1})$$

while the inverse Fourier transform is defined as

$$f(x) = \frac{1}{2\pi} \int_{-\infty}^{\infty} \hat{f}(\omega)e^{i\omega x} d\omega. \quad (\text{B2})$$

From Eq.(11) in the main article, we firstly need to find the time derivative of $\epsilon(t)$:

$$\frac{d\epsilon(t)}{dt} = -\frac{1}{2\pi} \int_0^\infty \int_0^{\omega_D} \frac{A\rho(\omega_p)e^{i\omega t}}{\omega^2 - (C\omega_p)^2 - i\omega\nu/m} d\omega_p d\omega \quad (\text{B3})$$

by using Eq.(11). We can change the order of integration, which gives:

$$\int_0^{\omega_D} A\rho(\omega_p) \int_0^\infty -\frac{1}{2\pi} \frac{e^{i\omega t}}{\omega^2 - (C\omega_p)^2 - i\omega\nu/m} d\omega d\omega_p.$$

Note that, for the inner integration, i.e., $\int_0^\infty -\frac{1}{2\pi} \frac{e^{i\omega t}}{\omega^2 - (C\omega_p)^2 - i\omega\nu/m} d\omega$, we could make an analytic continuation of ω to the complex plane and use contour integration to evaluate the Bromwich integral. However, we can achieve the same result via a simpler route just using the Fourier inversion theorem [42] that we recall below.

Theorem (The Fourier Inversion Theorem). *Suppose f is integrable and piecewise continuous on \mathbb{R} , defined at its points of discontinuity so as to satisfy $f(x) = \frac{1}{2}[f(x-) + f(x+)]$ for all x . Then $f(x) = \lim_{\epsilon \rightarrow 0} \frac{1}{2\pi} \int e^{-i\xi x} e^{-\epsilon^2 \xi^2 / 2} \hat{f}(\xi) d\xi$, $x \in \mathbb{R}$. Moreover, if $\hat{f} \in L^1$, then f is continuous and $f(x) = \frac{1}{2\pi} \int e^{-i\xi x} \hat{f}(\xi) d\xi$, $x \in \mathbb{R}$.*

The uniqueness of the inverse Fourier transform is guaranteed by this theorem. If we can find a function of time, whose Fourier transformation gives back the complex dielectric function $\epsilon^*(\omega)$, then this function would be the time derivative of the dielectric relaxation $\epsilon(t)$.

We use the following ansatz

$$\frac{e^{-\gamma t} \sin(Kt)}{K} H(t) \quad (\text{B4})$$

where $\gamma = \frac{\nu}{2m}$ and $K = \sqrt{-\frac{\nu^2}{4m^2} + (C\omega_p)^2}$ and $H(t)$ is a Heaviside step function, whose Fourier transformation is expressed as $\frac{1}{\omega^2 - i\nu\omega/m - (C\omega_p)^2}$.

However, we need to put care in taking $\nu \gg 2mC\omega_D$, which amounts to restricting our analysis to the high-friction overdamped dynamical regime. In this way, we finally obtain (for $t > 0$)

$$\frac{d\epsilon(t)}{dt} = e^{-\frac{\nu t}{2m}} \int_0^{\omega_D} \frac{A\rho(\omega_p) \sinh\left(\sqrt{\frac{\nu^2}{4m^2} - (C\omega_p)^2} t\right)}{\sqrt{\frac{\nu^2}{4m^2} - (C\omega_p)^2}} d\omega_p. \quad (\text{B5})$$

Upon further integrating over t , we recover Eq.(8) in the main article.

Appendix C: Behavior of ϵ when $\omega \rightarrow 0$

We take the limit $\omega \rightarrow 0$ in Eq. (1):

$$\begin{aligned} \lim_{\omega \rightarrow 0} \epsilon(\omega)^* &= \lim_{\omega \rightarrow 0} \left(1 - \int_0^{\omega_D} \frac{A\rho(\omega_p)}{\omega^2 - i(\nu/m)\omega - C^2\omega_p^2} d\omega_p \right) \\ &= 1 - A \cdot \lim_{\omega \rightarrow 0} \int_0^{\omega_D} \frac{\rho(\omega_p)}{\omega^2 - i(\nu/m)\omega - C^2\omega_p^2} d\omega_p \end{aligned} \quad (\text{C1})$$

We expand $\rho(\omega_p)$ around $\omega_p = 0$:

$$\rho(\omega_p) = \rho(0) + \rho'(0)\omega_p + \frac{\rho''(0)}{2}\omega_p^2 + \frac{\rho^{(3)}(0)}{6}\omega_p^3 + \dots \quad (\text{C2})$$

Thus, after substituting E.q(C2) into E.q(C1), we have

$$\begin{aligned} \lim_{\omega \rightarrow 0} \epsilon(\omega)^* &= 1 - A \lim_{\omega \rightarrow 0} \int_0^{\omega_D} \frac{\rho(0) + \rho'(0)\omega_p + \frac{\rho''(0)}{2}\omega_p^2 + \frac{\rho^{(3)}(0)}{6}\omega_p^3 + \dots}{\omega^2 - i(\nu/m)\omega - C^2\omega_p^2} d\omega_p \\ &= 1 - A \lim_{\omega \rightarrow 0} \int_0^{\omega_D} \frac{(\rho(0) + \rho'(0)\omega_p + \frac{\rho''(0)}{2}\omega_p^2 + \frac{\rho^{(3)}(0)}{6}\omega_p^3 + \dots)(\omega^2 + i(\nu/m)\omega - C^2\omega_p^2)}{\omega^4 - 2\omega^2\omega_p^2 + \omega_p^4 + \omega^2\nu^2/m^2} d\omega_p \\ &= 1 - A \lim_{\omega \rightarrow 0} \int_0^{\omega_D} \frac{W_0(\omega) + W_1(\omega)\omega_p + W_2(\omega)\omega_p^2 + W_3(\omega)\omega_p^3 + \dots}{\omega^4 - 2\omega^2\omega_p^2 + \omega_p^4 + \omega^2\nu^2} d\omega_p \end{aligned} \quad (\text{C3})$$

where $W_0(\omega) = \rho(0)(\omega^2 + i\nu/m\omega)$, $W_1(\omega) = \rho(0)'(\omega^2 + i\nu/m\omega)$, $W_2(\omega) = -\rho(0)C^2 + \frac{\rho^{(0)''}}{2}(\omega^2 + i\omega)$, $W_3(\omega) = \frac{(\omega^2 + i\nu/m\omega)\rho^{(3)}(0)}{6} - C^2\rho'(0)$. In order to let the integrand continuous on for both real and imaginary part, $(\omega, \omega_p) \in \mathcal{R}^+ \cup \{0\} \times \mathcal{R}^+ \cup \{0\}$ (then it makes sense to change the order of integration/limit at $(0,0)$), we must have $\rho(\omega_p) \sim 0$, $\rho'(\omega_p) \sim 0$, $\rho''(\omega_p) \sim 0$, $\rho^{(3)}(\omega_p) \sim 0$ as $\omega_p \rightarrow 0$. There is no restriction for $\rho^{(4)}(\omega_p)$ or higher order as $\omega_p \sim 0$.

Hence, we must have $\rho(\omega_p) \sim \omega_p^n$ for $n > 3$. In order to get linear scaling for ϵ' , we can let $\rho(\omega_p) \sim \omega_p^4$, then from E.q(C3), we actually want to know the behavior of

$$\lim_{\omega \rightarrow 0} \int_0^{\omega_D} \frac{\omega_p^4}{\omega^2 - i\nu/m\omega - C^2\omega_p^2} d\omega_p. \quad (\text{C4})$$

- [1] E. Donth, *The Glass Transition - Relaxation Dynamics in Liquids and Disordered Materials* (Springer, Berlin, 2001).
- [2] K. L. Ngai, *Relaxation and Diffusion in Complex Systems* (Springer, New York, 2011).
- [3] M. Fuchs, W. Goetze, I. Hofacker, A. Latz, *Comments on the alpha-peak shapes for relaxation in supercooled liquids*, J. Phys.: Condens. Matter 3, 5047 (1991).
- [4] *Complex Dynamics of Glass-Forming Liquids: A Mode-Coupling Theory* (Oxford University Press, Oxford, 2008).
- [5] R. Richert, *Supercooled liquids and glasses by dielectric relaxation spectroscopy*, Adv. Chem. Phys. 156, 101 (2015).
- [6] H. Yoshino and F. Zamponi, *Shear modulus of glasses: Results from the full replica-symmetry-breaking solution*, Phys. Rev. E 90, 022302 (2014).
- [7] H. Yoshino and M. Mezard, *Emergence of Rigidity at the Structural Glass Transition: A First-Principles Computation*, Phys. Rev. Lett. 105, 015504 (2010).
- [8] H. Yoshino, *Replica theory of the rigidity of structural glasses*, 136, 214108 (2012).
- [9] H. Froehlich, *Theory of Dielectrics* (Clarendon Press, Oxford, 1958).
- [10] C. J. F. Boettcher, *Theory of Electric Polarization* (Elsevier, Amsterdam, 1993).
- [11] M. Born and E. Wolf, *Principles of Optics* (Cambridge Univ. Press, Cambridge, 1999).
- [12] M. Born and K. Huang, *Dynamical theory of crystal lattices* (Oxford Univ. Press, Oxford, 1952).
- [13] M. Cardona et al., *Comment on the history of the stretched exponential function*, arxiv.org/pdf/0710.4446 (2007).
- [14] G. Williams and D.C. Watts, *Non-symmetrical dielectric relaxation behaviour arising from a simple empirical decay function*, Trans. Faraday Soc. 66, 80 (1970).
- [15] J.C. Phillips, *Stretched exponential relaxation in molecular and electronic glasses*, Rep. Prog. Phys. 59 (1996).
- [16] P.G. de Gennes, *Relaxation anomalies in linear polymer melts*, Macromolecules, 35:3785-3786 (2002)
- [17] M. Schwartz and S.F. Edwards, *Stretched exponential in non-linear stochastic field theories*, Physica A, 312, 363-368, (2002)
- [18] R. Milkus and A. Zacccone, *Local inversion-symmetry breaking controls the boson peak in glasses and crystals*, Phys. Rev. B 93, 094204 (2016).
- [19] W. Schirmacher, G. Ruocco, and T. Scopigno, *Acoustic Attenuation in Glasses and its Relation with the Boson Peak*, Phys. Rev. Lett. 98, 025501 (2007).
- [20] H. Shintani and H. Tanaka, *Universal link between the boson peak and transverse phonons in glass* Nature Mater. 7, 870 (2008).
- [21] L.E. Silbert, A. J. Liu, S.R. Nagel, *Vibrations and Diverging Length Scales Near the Unjamming Transition* Phys. Rev. Lett. 95, 098301 (2005).
- [22] M. L. Manning and A. J. Liu A random-matrix definition of the boson peak EPL 109, 36002 (2015).
- [23] A. Widmer-Cooper, H. Perry, P. Harrowell, D. R. Reichman *Irreversible reorganization in a supercooled liquid originates from localized soft modes*, Nature Phys. 4, 711 (2008).
- [24] W. Schirmacher, G. Ruocco, V. Mazzone *Heterogeneous Viscoelasticity: A Combined Theory of Dynamic and Elastic Heterogeneity*, Phys. Rev. Lett. 115, 015901 (2015).
- [25] M. Guerdane and H. Teichler *Short-Range-Order Lifetime and the Boson Peak in a Metallic Glass Model*, Phys. Rev. Lett. 101, 065506 (2008).
- [26] Yu.P. Mitrofanov, M. Peterlechner, S.V. Divinski, G. Wilde *Impact of Plastic Deformation and Shear Band Formation on the Boson Heat Capacity Peak of a Bulk Metallic Glass*, Phys. Rev. Lett. 112, 135901 (2014).
- [27] P. Lunkenheimer, U. Schneider, R. Brand and A. Loidl, *Glassy Dynamics*, Contemporary Phys. 41, 1 (2000).
- [28] A. Zacccone and E. M. Terentjev, *Disorder-assisted melting and the glass transition of amorphous solids*, Phys. Rev. Lett, 110, 178002 (2013).
- [29] P. Lunkenheimer, A. Pimenov, B. Schiener, R. Boehmer, and A. Loidl, *High-frequency dielectric spectroscopy on glycerol*, Europhys. Lett., 33, (1996).
- [30] M. Paluch, K.L. Ngai and S.H. Bielewka, *Pressure and temperature dependences of the relaxation dynamics of cresolphthalein-dimethylether: Evidence of contributions from thermodynamics and molecular interactions*, J. Chem. Phys. 114, 10872 (2001).
- [31] U. Schneider, R. Brand, P. Lunkenheimer and A. Loidl, *Excess wing in the dielectric loss of glass formers: a Johari-Gostein β relaxaion?*, Phys. Rev. Lett. 84, 5560 (2000).
- [32] A. Dob, M. Paluch, H. Sillescu and G. Hinze, *From strong to fragile glass formers: Secondary relaxation in polyalcohols*, Phys. Rev. Lett. 88, 095701 (2002).
- [33] J. Mattsson, R. Bergman, P. Jacobsson and L. Boerjesson, *Chain-Length-Dependent relaxation scenarios in an oligomeric glass-forming system: from merged to well-separated α and β loss peaks*, Phys. Rev. Lett. 90, 075702 (2003).
- [34] T. Blochowicz and E.A. Roessler, *Beta relaxation versus high frequency wing in the dielectric spectra of a binary molecular glass former*, Phys. Rev. Lett. 92, 225701 (2004).
- [35] The response in the time domain is related to the response in the frequency domain [36]
- $$\begin{aligned} \epsilon^*(\omega) &= \epsilon'(\omega) - i\epsilon''(\omega) \\ &= \epsilon^*(\infty) + (\epsilon^*(\infty) - \epsilon^*(0)) \int_0^\infty e^{-i\omega t} \frac{d\phi}{dt} dt. \end{aligned} \quad (5)$$
- The relaxation function is related to the response in the time domain via [36]:
- $$\begin{aligned} \epsilon(t) &= \epsilon^*(\omega = \infty) + \\ &(\epsilon^*(\omega = 0) - \epsilon^*(\omega = \infty))(1 - \phi(t)) \end{aligned} \quad (6)$$
- where $\phi(t) = \exp[-(t/\tau)^\beta]$. Predictions of this equation have also been plotted for comparison in Fig. 2-3, for the frequency-dependent response, and in Fig. 4 for the time-dependent response, together with the predictions of our theory. Note that the parameters in the Kohlrausch model have been also adjusted to match with the experimental data.

- [36] E. W. Montroll and J. T. Bendler, *On Levy (or Stable) Distributions and the Williams- Watts Model of Dielectric Relaxation*, J. Stat. Phys. 34, 129 (1983).
- [37] Supplementary information available at (1999)
- [38] J.P. Garrahan and D. Chandler, *Geometrical Explanation and Scaling of Dynamical Heterogeneities in Glass Forming Systems*, Phys. Rev. Lett. 89, 035704 (2002).
- [39] D.J. Ashton and J.P. Garrahan, *Relationship between vibrations and dynamical heterogeneity in a model glass former: Extended soft modes but local relaxation*, Eur. Phys. J. E 30, 303?307 (2009).
- [40] T. C. Choy, *Effective Medium Theory: Principles and Applications* (Oxford University Express, 2016, New York).
- [41] W. Jones and N. H. March, *Theoretical Solid State Physics* (Wiley-Interscience, 1973, John Wiley & Sons London).
- [42] G.B. Folland, *Fourier Analysis and its Applications* (Wadsworth, Belmont, California, 1992).